Journal of Chromatography A, 1236 (2012) 152–163

Contents lists available at SciVerse ScienceDirect

Journal of Chromatography A

journal homepage: www.elsevier.com/locate/chroma

On the chromatographic efficiency of analytical scale column format porous polymer monoliths: Interplay of morphology and nanoscale gel porosity

Ivo Nischang*

Institute of Polymer Chemistry, Johannes Kepler University Linz, Welser Strasse 42, A-4060 Leonding, Austria

ARTICLE INFO

Article history:
Received 28 December 2011
Received in revised form 3 March 2012
Accepted 5 March 2012
Available online 10 March 2012

Keywords:
Adsorption
Chromatographic performance
Cross-linked polymers
Efficiency
Feature size
Gel porosity
Mass transfer
Monolith
Pore heterogeneity
Partition
Plate height
Porous polymers
Retention
Reversed-phase
Spatial inhomogeneity

ABSTRACT

Porous monolithic poly(styrene-*co*-divinylbenzene) stationary phases in 4.6 mm I.D. analytical-scale column format with varying porosity, globule scale polymer morphology and flow-through pore structure have been investigated with respect to their transport properties toward small retained solutes in isocratic elution, reversed-phase liquid chromatography. The current study was performed under kinetically and thermodynamically relevant conditions comprising retention factors from close to zero up to the order of 50–100 under most extreme conditions, while a linear chromatographic flow velocity up to 4 mm/s, in some instances up to 7 mm/s, was realized. Carefully designed experiments aimed at resolving issues associated with the monoliths performance, while a particular focus is given on gel porosity, chromatographic retention and band dispersion. Elucidation of three important metric properties gave orthogonal insight. These are: (i) the columns dry-state morphology and surface area, (ii) the gel porosity with tetrahydrofuran as solvent determined by size exclusion chromatography using a range of small subnanometer-sized molecules and polystyrene standards, as well as (iii) the isocratic reversed-phase performance of small molecules at varying binary acetonitrile/water mobile phase solvent compositions, modulating gel porosity. Consistently throughout the study, the adjustable and general retention-factor-dependence of the performance of these monolithic materials is shown. It can also be correlated to the analytes molecular weight and consequently size. Isocratic performance strongly depends on the amount of gel porosity of the scaffold, which can be changed by varying the percentage of organic modifier in the mobile phase and indicates the adjustable chromatographic nature of porous polymer monoliths. This gel porosity which is absent in the dry-state of the polymer monoliths and is characterized by sub-nanometer to nanometer-sized pore space induces, additionally to permanent porosity, stagnant mass transfer zones. The displayed major reason for mass transfer resistance implied by the use of polymeric monolithic columns determines dispersion behavior of small molecules and its varying importance with respect to morphology and size of the globular features containing stagnant mass transfer zones is addressed. This leads to the conclusion, that a reduction in polymer feature size and increase in number of flow-through pores per unit cross-section of the monolith with an improved homogeneity may be an interesting option of tailoring column performance. It is further concluded that dry-state methods (such as nitrogen adsorption analysis and scanning electron microscopy) or solvated-state methods (such as size-exclusion chromatography in tetrahydrofuran) by itself are insufficient measures to explain the adjustable chromatographic performance of porous polymer monoliths.

1. Introduction

Since the inception of porous polymer monolithic column technology, their conceptual success was associated with enhanced mass transfer in the typically micrometer-sized flow-through pore space that may potentially lead to faster and more efficient separations [1–3]. This has in particular mostly been demonstrated by large molecule separations in gradient elution mode chromatography and later that of nucleic acids and of peptides found in proteomic samples [3–6]. The conceptual success of the polymer monoliths in such scenarios of non-equilibrium elution modes is attracting an ever increasing amount of potential users in particular in the bio-analytical arena dealing with the analysis of proteolytic digests or large biomolecular species [7–9]. The preparation of porous polymer monoliths is well documented [10] and the versatility stemming from the arsenal of chemistries used during their preparation with varying initiating systems or in post-polymerization grafting-steps is steadily increasing [11]. However, many of the new methods resulting in monolithic entities have not found their way to the chromatographic arena.

* Tel.: +43 732 671547 66; fax: +43 732 671547 62.
E-mail address: ivo.nischang@jku.at

0021-9673/$ – see front matter © 2012 Elsevier B.V. All rights reserved.
doi:10.1016/j.chroma.2012.03.017

In particular, with the recent shift to microfluidic chip formats in chromatography, microscale separation formats employing capillaries with small inner diameters of <50 μm [12–14], and as recently emerged thin layers [15], important stepping stones for the use of commonly employed and easily implementable free-radical processes have been established.

In general, the morphological situation and porous properties of polymer-based monolithic separation media prepared in a single-step molding process, involving thermally or radiation-initiated free radical polymerization reactions, is readily peculiar. In a first approximation, polymer monoliths consist of polymer globules and their agglomerates forming a three-dimensionally adhered polymer backbone intertwined by micrometer-sized pores. Such structure, being the most typical, originates from the free-radical processes used in their preparation [16,17]. However, as a fundamental property, the porous monoliths in liquid chromatography are separation media which show micrometer-sized flow through pores (just as a packed bed of adsorbent particles or silica-based monoliths) and a variable microporous/mesoporous backbone structure with a stagnant mass transfer zone in which (hindered) diffusion prevails. This may not be indicated in the dry, non-solvated state [18]. It was shown, that this is most pronounced for molecules that fit into pores of the developed gel porosity on a nanometer-scale, while the overall macroscopically accessible transport performance is impacted by convective flow dispersion, as well as diffusion, partitioning in and adsorption on the polymeric globule-scale matrix [18,19]. Phenomenologically, this can be evidenced by the mass transfer contribution (classically *C*-Term contribution) to the plate height of small molecules impacted by analyte size and retention often observed in the chromatographic characterization of polymer monoliths [18–21]. Along this line, we suggested the concept of gel porosity as an indispensable tool explaining performance of porous polymer monoliths including that of retention-dependent dispersion phenomena [18]. However, the metric properties of this gel porosity and its particular impact on analyte transport have only been indirectly addressed with reversed-phase chromatographic studies of small molecules [18,19].

Analytical column scale formats are still the dominating formats used in the pharmaceutical industries due to robustness provided for process control operations and to ensure product quality. While initial studies with polymer monoliths in analytical column format showed less success in their performance for small molecule applications [23], the materials format underwent a rapid transition toward miniaturization and has conquered the field of nano-liquid chromatography and microfluidics [12]. However, commonalities of larger inner diameter analytical monolithic columns and their smaller sized counterparts with respect to performance have not been well described in the current literature. Their success in miniaturized column format may be due to the easily implementable processes allowing preparation of porous adsorbent media, again with an outstanding versatility of chemistries during copolymerization or post-polymerization grafting. Most efforts in improving the performance in the capillary-scale format have appeared in the literature and also increasingly focus on the small molecule arena, for which the materials have not been developed originally [18,19,24–28]. Further, recent studies also have the 3 mm I.D. [29] and 1 mm I.D. [30] column format as an objective. However, independently from the vanished, though still existent, attention to a larger scale column format and recent shift to microfluidic formats, understanding of flow and transport still remains an important challenge. This understanding should, as an ultimate goal, lead to a structure-directed synthesis mediating for the most important reasons that limit column performance and therefore allow accessibility to a broader application range including small molecules. While in typical microfluidic conduits the monolithic structures are covalently anchored to the confining container [12], preparation in larger, even preparative column formats may significantly impart problems due to orders of magnitude smaller surface-to-volume ratio molds. This may affect the ease of integration ability of these structures [31,32]. The preparation of polymer monoliths in larger diameter molds involves development of possible radial temperature gradients that influence local free-radical reaction dynamics potentially contributing to axial or lateral heterogeneities in the monolithic structures [32]. These may be less pronounced in microfluidic conduits [33] until wall effects from the confining container markedly influence the porous structure at further miniaturization [14].

In this experimental study the transport and performance characteristics of porous polymer monoliths in analytical-scale column format based on styrene/divinylbenzene chemistry is explored. These materials have been developed for high throughput protein and peptide analysis. In the current work, a careful choice of different metric properties of the stationary phase under rather untypical conditions for which it was optimized is selected. The aim is to gain most fundamental insight on macroporous flow-through-pore structure and nanoscale gel porosity of the monoliths. The current study includes investigations on the dry-state specific surface area, size exclusion chromatography in thermodynamically good solvent tetrahydrofuran to determine gel porosity under such conditions, and chromatographic investigations in the reversed-phase chromatographic transport properties probed by small molecules. The chromatographic properties are investigated under conditions of strong and weak retention that imply modulation of gel porosity.

2. Experimental

2.1. Chemicals and materials

Uracil, alkylbenzenes, PS-standards with a narrow molecular weight distribution, HPLC-grade tetrahydrofuran, and acetonitrile were purchased from Sigma–Aldrich (Vienna, Austria). The polystyrene (PS) standards have a molecular weight, M_w, of 436, 1110, 3250, 9500, 20,000, 35,000, 65,000, 154,000, 200,000, 600,000, 900,000, and 2,000,000 g/mol. Water was purified on a Milli-Q Reference water purification system from Millipore (Vienna, Austria). Sample solutions were prepared in running mobile phases containing various volume percentages of acetonitrile/water (v/v) for reversed-phase liquid chromatography experiments, or in tetrahydrofuran for size exclusion chromatography (SEC) experiments.

2.2. Equipment, chromatographic measurements, and columns

Chromatographic measurements were performed on a 1290 Infinity UPLC system (Agilent Technologies, Vienna, Austria) without major modifications and narrow bore connecting stainless steel capillaries resulting in ≤5% extra-column volume of the nominal 4.6 mm × 50 mm column dimensions. Therefore external contributions to band broadening have not been considered in this comparative work, however the extra-column volume has been considered for the calculation of the monoliths porosity from elution studies. Injection of 1 μl sample has been performed in all experiments and UV-detection was carried out at a wavelength of 210 nm. Unless otherwise stated, chromatographic experiments have been carried out at a controlled temperature of 25 °C.

In this study, a set of three commercially available poly(styrene-*co*-divinylbenzene) monolithic stationary phases in 4.5 mm I.D. stainless steel housing have been investigated. They are available under the trade name ProSwift, while advertised and optimized for high performance protein separations in reversed-phase gradient

mode, but here used in combination with a homologous series of alkylbenzenes. The exact bed dimensions were 4.6 mm × 46 mm for the RP1S, 4.6 mm × 44 mm for the RP2H, and 4.6 mm × 40 mm for the RP3U column. The monoliths were a kind gift from Thermo Fisher Scientific (Sunnyvale, CA) as research samples. After conditioning the columns with acetonitrile with at least 30 column volumes, they were equilibrated with the desired binary mobile phase solvent composed of varying percentages of acetonitrile and water before evaluating the reversed-phase isocratic performance in the elution of a homologous series of alkylbenzenes. In some experiments high temperature liquid chromatography was utilized making use of the variable temperature column oven configuration of the 1290 Infinity.

For SEC, tetrahydrofuran was used as the mobile phase at a flow rate of 0.3 ml/min and a controlled temperature of 25 °C. Injection of the respective analytes, that were a homologous series of alkylbenzenes from benzene to pentylbenzene and narrow molecular weight distribution PS standards, was performed in triplicate and average values are reported.

Nitrogen adsorption experiments to determine the columns dry-state surface area were performed with a Micromeritics TriStar II Surface Area and Porosity Instrument (SY-LAB Geräte GmbH, Neu-Purkersdorf, Austria). Dry-state surface areas were calculated based on the Brunauer–Emmett–Teller (BET) equation.

Scanning electron micrographs were obtained using a Crossbeam 1540 XB electron microscope (Carl Zeiss SMT AG, Oberkochen, Germany).

2.3. Simple metrics of characterization

In chromatography, we can define a tracer-porosity, ε_{tracer}, by simple relation of a tracer elution volume, V_{el}, to the geometrical volume of the column, V_{col}:

$$\varepsilon_{tracer} = \frac{V_{el}}{V_{col}} \quad (1)$$

which, in the absence of adsorption and partition leads to the pore space experienced by a tracer at the given mobile phase solvent composition. The porosity probed with a totally permeating non-interacting small tracer (ε_{total}) can be used to define a phase ratio:

$$\Phi = \frac{1 - \varepsilon_{total}}{\varepsilon_{total}} \quad (2)$$

with the benzene in SEC and uracil in reversed-phase chromatography assumed as the smallest eluted compounds in the current study.

In SEC, and when comparing different columns that vary in porosity but have identical backbone chemistry, we can use the elution volume of a totally permeating smallest marker, V_{el}, as a reference to that of analytes of an increased size, $V_{el,tracer}$. This leads to a normalized elution volume, $V_{el,n}$:

$$V_{el,n} = \frac{V_{el,tracer}}{V_{el}} \quad (3)$$

The results then always show that the benzene as smallest compound in SEC has a $V_{el,n}$ equal to one while larger tracers may only see a part of this pore volume since they are increasingly excluded from the available pore space that is seen by benzene.

Alternatively to Eq. (1), ε_{total}, can be determined at any mobile phase composition from the ratio of superficial flow velocity, u_{sf}, and linear chromatographic flow velocity, u_0, determined from the elution time of a non-retained small tracer which may be assumed to permeate all available pore space at the specific mobile phase composition [33,34]:

$$\varepsilon_{total} = \frac{u_{sf}}{u_0} \quad (4)$$

where the superficial flow velocity, u_{sf}, is the ratio of flow rate, F_v, and cross-sectional area of the column, A, and u_0 the ratio of elution time of non-retained tracer, t_0, and length of the column, L. The superficial velocity-based hydrodynamic permeability, $k_{p,f}$, can be defined as [34]:

$$k_{p,f} = \frac{L}{\Delta P} \eta u_{sf} \quad (5)$$

where ΔP is the pressure drop and η is the mobile phase viscosity. Since the connecting capillary tubings had a diameter of only 120 μm I.D. as opposed to the 4.5 mm I.D. column format we first measured the system pressure with a polymer monolithic column in the flow path of the system. After measurements, the pressure generated by the capillary connections in the LC instrument was determined at the same flow rate. This allowed the determination of backpressure generated by the respective monolithic column and therefore the permeability.

3. Results

3.1. Microscopic structure and dry-state porous properties

Most widely means of characterizing the dry-state porous structure of polymer monoliths integrated into chromatographic conduits has been that of scanning electron microscopy (SEM). Fig. 1 shows the example cross-sectional microscopic structure of the poly(styrene-*co*-divinylbenzene) porous polymer monoliths encased in the 4.5 mm I.D. chromatographic conduits. The typical macroporous structure composed of irregularly sized and interadhered globules is apparent as well as the significant difference between all three investigated columns with a trend in the microscopic architectures from Fig. 1a–c. The size of the individual globular features of which the monolithic backbone is composed is largest for the RP3U series (Fig. 1a), while they are significantly smaller and with a larger population for the RP2H (Fig. 1b) and RP1S series (Fig. 1c). This is in conjunction with a larger amount of flow-through channels of smaller size per unit cross-section from Fig. 1a–c. The smaller size of the individual globular features may already indicate a higher dry-state surface area of the porous monoliths RP2H (Fig. 1b) and RP1S (Fig. 1c) while it may be lowest for that of the RP3U (Fig. 1a). It is further apparent that all monoliths are microscopically heterogeneous with limited self-similarity and therefore reflect random porous media composed of cross-linked polymer globules. However, their nanometer-sized structure does not become resolvable in the dry, non-solvated state under present conditions. The structure needs to be further characterized by isocratic elution of small molecules [18].

Nitrogen adsorption experiments revealed significantly different dry-state BET surface areas of 1.2 m^2/g, 319 m^2/g, and 395 m^2/g confirming the fact that the dry-state specific surface area increases according to RP3U < RP2H < RP1S (Fig. 1a–c, Table 1). The increased surface area for the RP1S column may have its reason in the smaller globule size and smaller voids in between them as well as possibly a higher degree of cross-linking (Fig. 1c) [17]. It is therefore concluded that the expected total surface areas of the porous polymeric materials may be an important anchor for further investigations. Unfortunately, surface area measurements alone do not allow for rational conclusions on their chromatographic performance in the typical hydro-organic solvents used in liquid chromatography that results in solvation and nanoscale swelling of the scaffold structures [17].

3.2. Inverse size exclusion chromatography and gel porosity

Recent investigations on porous polymer monoliths, their formation, development of porous properties in due course

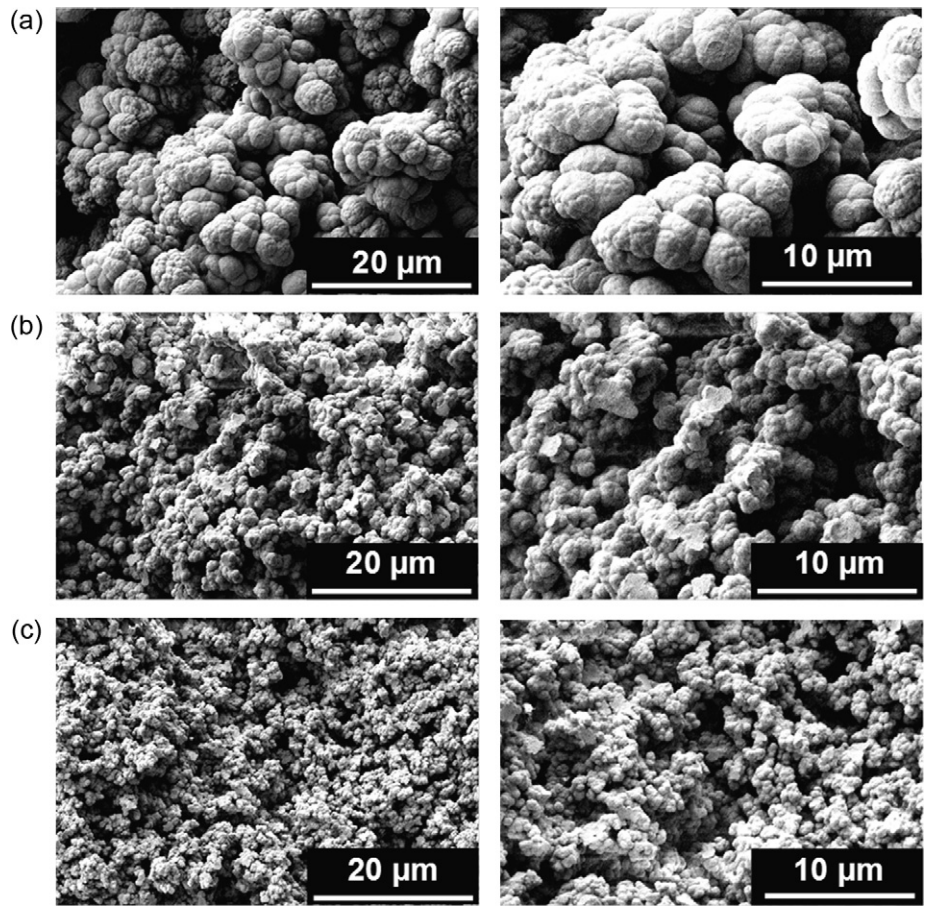

Fig. 1. Example scanning electron microscopy images of the bulk region of monolithic poly(styrene-*co*-divinylbenzene) stationary phases in 4.6 mm I.D. analytical column format with (a) the RP3U, (b) the RP2H, and (c) the RP1S series at different magnifications.

of polymerization and isocratic reversed-phase performance in capillary-scale format revealed that they are composed of heterogeneously cross-linked polymer systems which are susceptible to develop gel porosity in contact with solvent [18,19]. It was suggested that this contact with solvent liberates nanometer-sized pore space, making the presumably pore confining polymer probed in the dry-state accessible to molecules that are small enough to fit into the gel pores. Consequently, analyte dispersion through the monolithic material is, additionally to convective flow dispersion, affected by (hindered) diffusive contributions to and from the active adsorption sites located in and on the globular structures. Analyte dispersion is therefore strongly impacted by this stagnant mass transfer resistance in the polymer globule structures and becomes significant in particular at increased linear chromatographic flow velocities, i.e. the regime dominated by mass transfer resistance contributions to the plate height [17]. The complexity of this type of contributions to the height equivalent to the theoretical plate was anchored to the conceptual property gel porosity used by Jerabek in the characterization of polymeric bead-based separation media [17,18,35]. Gel porosity is a porosity which stems from solvation and swelling of cross-linked polymer and refers to the pore space within the structure of the solvated stationary phases, not the dry [17,18,35]. The gel pores of monoliths are suspected to measure less than ten nanometers, in particular measure smaller than a single nanometer and their pore volume and size depends on the degree of cross-linking [17,35] and solvents used in chromatographic applications [35–37]. Since these gel pores are located in the intra-globular zones in the monolithic chromatographic bed in which molecules in the order of sizes of these pores can partition, respectively diffuse, an attempt is made to show this gel porosity

Table 1
Porous properties of the poly(styrene-*co*-divinylbenzene) polymer monoliths investigated in this study.

Column	ε_{total} [a]	ε_{tracer} [b]	ε_{tracer} [c]	Φ [d]	ε_{total} [e]	Φ [f]	$k_{p,f}$ [g] [10^{-14} m^2]	A_s [h] [m^2/g]
RP3U	0.528	0.434	0.375	0.89	0.484	1.07	7.1	1.2
RP2H	0.602	0.507	0.443	0.66	0.544	0.84	3.4	323
RP1S	0.612	0.530	0.415	0.63	0.559	0.79	1.2	395

[a] Porosity according to the permeation volume of benzene in SEC using tetrahydrofuran as mobile phase after Eq. (1).
[b] Porosity according to the permeation volume of the smallest PS standard (M_w = 436 g/mol) in SEC using tetrahydrofuran as mobile phase after Eq. (1).
[c] Porosity according to the permeation volume of the largest PS standard (M_w = 2,000,000 g/mol) in SEC using tetrahydrofuran as mobile phase after Eq. (1).
[d] Phase ratio derived from the porosity probed with benzene in tetrahydrofuran after Eq. (2).
[e] Porosity calculated according to the ratio of superficial and linear chromatographic flow velocity measured in 50/50 acetonitrile/water (v/v) as mobile phase after Eq. (4).
[f] Phase ratio from non-retained uracil in 50/50 acetonitrile/water (v/v) as mobile phase after Eq. (2).
[g] Superficial-velocity-based hydrodynamic permeability determined with 50/50 acetonitrile/water (v/v) as the mobile phase after Eq. (5).
[h] Specific surface area calculated after Brunauer–Emmett–Teller (BET) from nitrogen adsorption data.

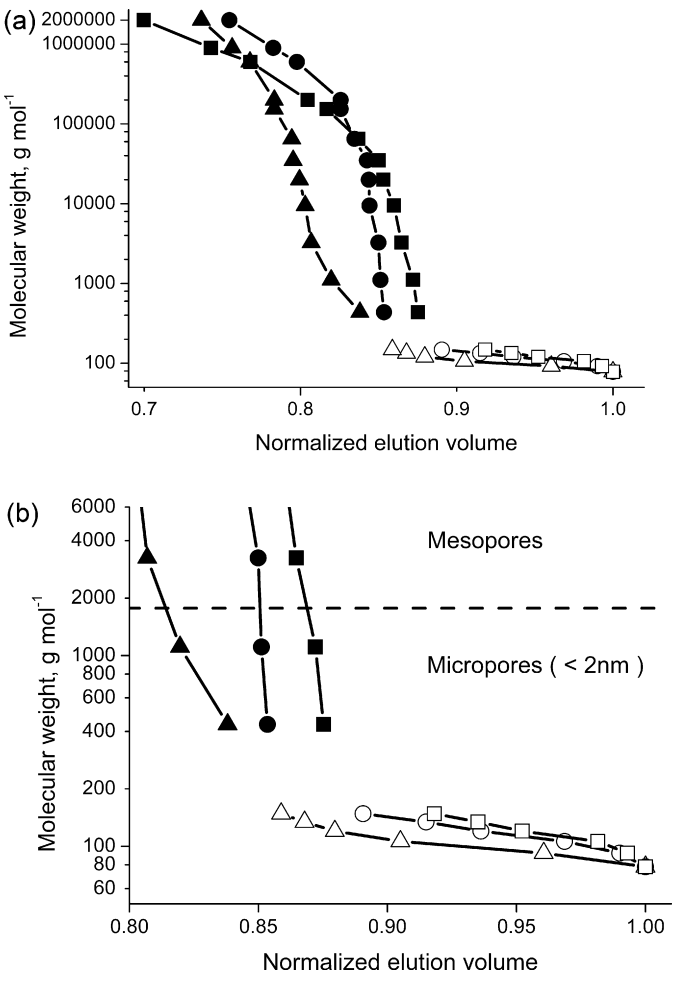

Fig. 2. Size exclusion chromatography curves derived from elution of small tracers and polystyrene (PS) standards in tetrahydrofuran and for the monolithic materials shown in Fig. 1 by relating (a) molecular weight of alkylbenzenes and molecular weight of PS standards (M_w) to normalized elution volume ($V_{el,n}$, Eq. (3)), and (b) zoom area focusing on the low molecular weight PS standards and alkylbenzenes. Dotted line indicates the molecular weight of the PS standard that would result in the respective hydrodynamic radius of 2 nm [38]. PS standards are shown by filled symbols and the homologous series of alkylbenzenes by open symbols. Symbol key: RP3U (triangles), RP2H (circles), (RP1S) squares.

for the current columns by the use of inverse SEC. A series of twelve PS standards and a homologous series of alkylbenzenes from benzene to pentylbenzene have therefore been employed. The good thermodynamic solvent tetrahydrofuran solvates the cross-linked polymer phase and presumably also suppresses interaction of the PS standards and the utilized small molecules with the polymeric matrix.

Fig. 2a shows SEC curves on all three monolithic columns in which the molecular weight of the PS standards, respectively small molecules, has been plotted against the normalized elution volume with the benzene assumed as the smallest totally permeating tracer (Eq. (3)). It is apparent that all three monoliths show relatively steep SEC curves for the PS standards. The total porosity with the PS standards ranging in molecular weight from M_w = 436 to 35,000 g/mol changes in the row RP3U < RP2H < RP1S, which can also be seen in Table 1. The RP2H and RP1S series are close to each other (Fig. 2a). The data in Fig. 2a show that a fraction of the pores for monolith RP1S with M_w larger than 35,000 g/mol is not accessible for the respective PS standards, while it is accessible for smaller polystyrene standards (M_w < 35,000 g/mol). This may be explained by the pore structure indicated in Fig. 1c. Larger analytes are excluded from part of the voids between the relatively small and fine globular structures for the RP1S column due to a related mesoporosity. However, all three stationary phases also display an amazingly high accessibility for small molecules depending on their size (open symbols for alkylbenzenes ranging from pentylbenzene (left) to benzene (right), Fig. 2). The relatively flat curve of the SEC profile shows size exclusion behavior of sub-nanometer sized molecules providing direct evidence for the nanoporous structure of the monoliths. Fig. 2b shows an enlarged view of the low molecular weight region for the PS standards and small alkylbenzenes used for chromatographic characterization of the monolithic materials (vide infra). The horizontal line reflects the molecular weight of a PS standard that has a hydrodynamic radius of 2 nm in tetrahydrofuran [38]. Focusing below the horizontal line in Fig. 2b and on the alkylbenzenes, one methyl group in toluene as opposed to benzene already results in a small difference in elution volume while the pentylbenzene elution volume is 14% smaller than the benzene elution volume for the RP3U series (Fig. 2b, open triangles). While this sized-based elution behavior indicates the existence of very small sub-nanometer sized pores, it is also seen that interaction with the stationary phase may be totally suppressed. The elution behavior in Fig. 2 is determined by size, with the largest (highest molecular weight) alkylbenzene eluting first and being closest to the nanopore exclusion limit. This is in contrast to its expected elution in reversed-phase liquid chromatography (vide infra).

Once again, the data in Fig. 2 reveal the relative accessibility of the polymeric matrices under conditions where partition is reduced to a minimum and indirectly reflects the accessibility of the column containing cross-linked polymer which is seen by both hydrodynamic flow and (hindered) diffusion of molecules of specific size. For all three columns, the strongest change in normalized elution volume is observed for molecular sizes below 2 nm, i.e. the alkylbenzenes. The RP3U column clearly has mesopores/micropores in solvent tetrahydrofuran though in the dry-state this column shows an apparent absence of small pores indicated by the SEM images (Fig. 1a) and a dry-state specific surface area of only 1.2 m^2/g (Table 1). For example considering the RP3U column, the smallest polystyrene standard of M_w = 436 g/mol sees only 84% of the porosity that is seen by the smallest analyte benzene. Considering all SEC curves in Fig. 2, it is safe to assume that the gel porosity is largest for the RP3U column followed by the RP2H column and the RP1S column. The RP1S column has the smallest gel porosity because it has the largest permanent porosity, largest dry-state specific surface area (Table 1), and the largest porosity seen by PS standards of $M_w \leq$ 35,000 g/mol (Fig. 2). In other words, the difference in elution volumes between the smallest PS standard and benzene is smallest for the RP1S column.

However, considering the size selectivity for small alkylbenzenes, the existence of nanometer-sized pores in contact with solvent is clear for all three monolithic columns. This is observed irrespective of their dry-state porous structure, morphology (Fig. 1), and surface area (Table 1). The results therefore indicate a general material characteristic of cross-linked polymer material forming the interstices through which the liquid convectively percolates. This most simple experiment ad hoc evidences that small molecules permeate the poly(styrene-*co*-divinylbenzene) matrix in the solvated swollen-state. Dry-state or typical size exclusion chromatographic investigations utilizing PS standards alone cannot probe for this porosity. Therefore in any instance the assumption of the absence of small pores and low surface area is invalid though it may be suggested by dry-state methods (Fig. 1 and Table 1). When mesopores are present in the dry-state, gel porosity additionally modulates the porous structure. Consulting the literature on porous polymeric bead-based materials, this shows that though the monolithic columns may reflect a porous entity morphologically different from that of their earlier generation bead-based materials, they show the same phenomenon of gel porosity and

possibly related partition and adsorption phenomena [39–42]. This most importantly reflects the typical framework opening in cross-linked polymer systems in their solvated swollen-state as a base material property [37], irrespective of the stationary phase morphology [17]. We should, however, recall that this is most often neglected in the discussion of their performance but was identified to have a large impact for retained small analytes [17]. It may be expected that this permeation of small tracers also holds under typical reversed-phase chromatographic conditions with varying binary mobile phase solvent compositions in which analyte partition, adsorption, and the existent gel porosity are modulated. The solvated nanoscale state of cross-linked polymer depends on the volume percentage and solvating properties of the organic modifier [17,36,37,39,40]. Since relevant data on porous polymer monoliths are scarce, if not absent, in the literature, the objective of the following experiments is to shed light on its impact toward analyte retention and chromatographic efficiency in reversed-phase liquid chromatography.

3.3. Chromatographic reversed-phase elution of small molecules and retention factor

In addition to the discussed differences in the porous structure between the swollen and dry-state we now move to a situation in which hydro-organic solvents, typical for reversed-phase chromatographic applications, are used. A composition of 50/50 acetonitrile/water (v/v) was chosen as a starting point. Fig. 3 shows the retention pattern of all three columns and indicates that the number of alkyl carbon atoms in the homologous series causes an increase in retention. All columns show a similar selectivity in the elution of alkylbenzenes at 50/50 acetonitrile/water (v/v) as mobile phase (circles in Fig. 3). Most interestingly the RP3U column with the lowest, barely measurable dry-state specific surface area shows strongest retention for alkylbenzenes. This is in accordance with the higher phase ratio and higher gel porosity determined from SEC (Fig. 2, Table 1). Therefore, even under these conditions retention can be related to the phase ratio of the monolithic columns, not the dry-state specific surface area (Table 1), since the small tracers permeate the nanoscopically cross-linked polymeric matrix (Fig. 2). This cannot be probed by PS standards. This supports findings with experiments in capillary-scale format poly(styrene-*co*-divinylbenzene) monolithic columns [19]. Once more, it shows most fundamentally that retention does not

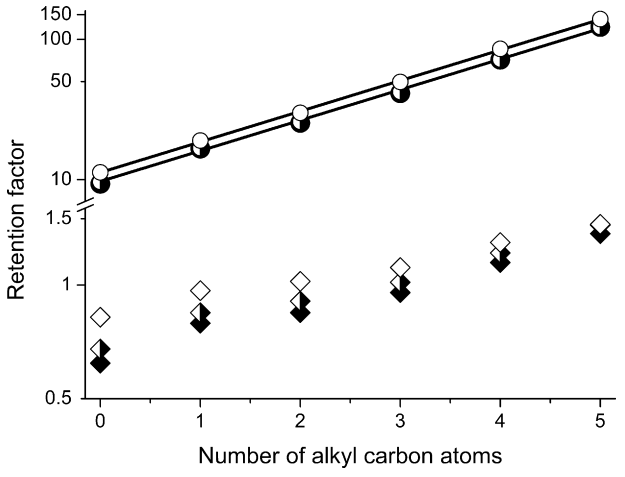

Fig. 3. Retention factor of alkylbenzenes against number of alkyl carbon atoms provided by the monolithic columns measured at a mobile phase composition of 50/50 acetonitrile/water (v/v) (circles) and only acetonitrile in the mobile phase (diamonds). Symbols: RP3U (open), RP2H (half-filled), RP1S (filled).

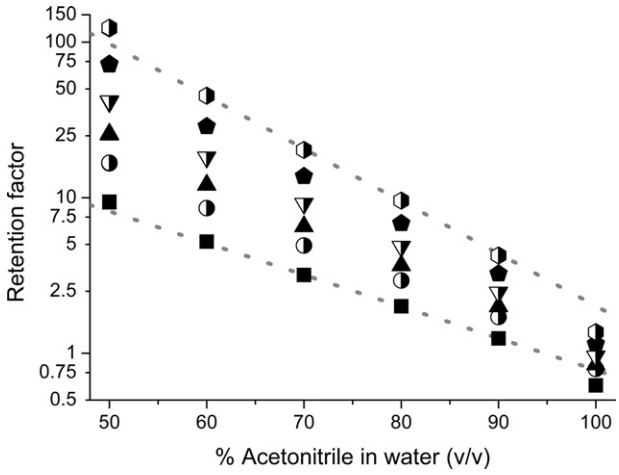

Fig. 4. Retention factors for the homologous series of benzene derivatives plotted against mobile phase composition and probed by utilizing the RP1S column for benzene (filled squares), toluene (half-filled circles), ethylbenzene (closed triangles), propylbenzene (half-filled triangles), butylbenzene (closed pentagons), and pentylbenzene (half-filled hexagons). Superficial flow velocity: 0.3 mm/s. Linear, dotted lines are shown only as a guide to the eye.

correlate with dry-state surface area and a similar selectivity is observed in all three cases (where the RP2H and RP1S series practically coincide). Shown also for all three columns, are the retention factors at a mobile phase composition comprising only acetonitrile, demonstrating that the slope of retention against number of alkyl carbon atoms becomes nonlinear. This indicates a variation of partition and adsorption [42], until elution behavior may purely resemble the one determined by size of the small molecules as in SEC employing tetrahydrofuran (Fig. 2).

To further elucidate this aspect, Fig. 4 shows the plot of retention for the homologous series against volume percentage of acetonitrile in the mobile phase for the RP1S column. The dotted lines shown in Fig. 4 are meant as a guide to the eye for the benzene and pentylbenzene data. Typically, only intermediate ranges of the volume fraction of organic modifiers are probed. For intermediate compositions, a linear behavior is seen while reasonable deviations are obvious at acetonitrile only and 50/50 acetonitrile/water (v/v) as the mobile phase (Fig. 4). Therefore, the variation of partition and adsorption has a concerted effect on the retention dynamics and becomes affected by the solvated state of the nanoscale polymer structure. However, it is well known that measured retention in linear chromatography cannot easily separate for partition and adsorption effects according to Gritti et al. [43]. They have shown that for a mixed retention mechanism on silica-based materials with contributions from different adsorption and/or partitioning sites, linear chromatography can only measure retention as the sum over all site types. In the present case the concerted contribution from partition in and adsorption onto the polymer matrix as opposed to its importance in the bonded layer of silica-based (meso)porous materials needs to be investigated [43–46].

3.4. Hydrodynamic dispersion of small molecules

In liquid chromatography, it is highly desirable to achieve performance and efficiency of elution at sufficiently high retention factors and under conditions of high selectivity. Therefore, the analysis is started with a mobile phase composition of 50/50 acetonitrile/water (v/v), realizing retention factors of close to 10 for benzene to more than 100 for pentylbenzene on all three columns (Fig. 3). Fig. 5 shows the plate height curves for pentylbenzene as the strongest retained compound (Fig. 3). It is obvious that the RP1S monolithic column performs best with a minimum plate height

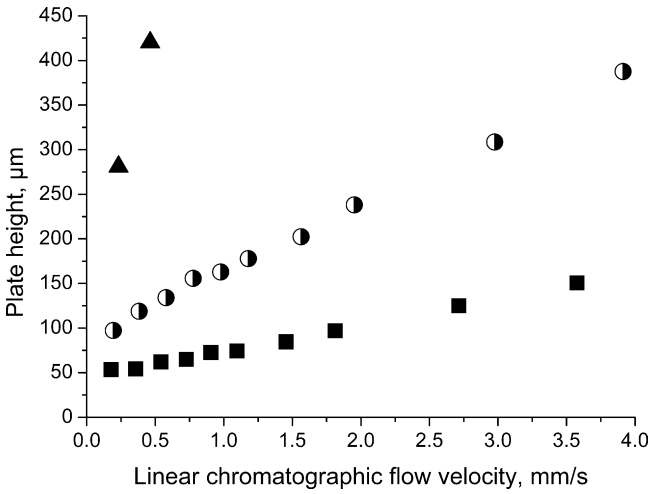

Fig. 5. Plate height curves obtained from the isocratic reversed-phase elution of strongly retained pentylbenzene on all three columns and a mobile phase composition of 50/50 acetonitrile/water (v/v). Symbols: RP1S (filled squares), RP2H (half-filled circles), RP3U (filled triangles).

of 50 μm, followed by the column RP2H with a plate height of 100 μm achieved at the lowest linear chromatographic flow velocity and with the RP3U performing worse and losing its efficiency most rapidly at increased linear chromatographic flow velocities. As we have seen from the previous analysis, indeed the column RP1S features the highest dry-state surface area (Table 1), and smallest average flow-through pore size at a finer globular structure (Fig. 1). Consequently, it also features the lowest permeability at this mobile phase composition (Table 1). The determined permeability data for all columns correlate well with the marked difference in porosity, globule and flow-through pore size (Fig. 1, Table 1). All these aspects may at first hand be responsible for the improved transport performance of small molecules provided by the RP1S column. However, judging from its characteristics of retention dynamics (Fig. 3), as well as associated selectivity, this dry-state surface area does not provide a significant increase in retention and selectivity as opposed to the other columns. For example, the dry-state specific surface area of the RP3U column is more than 300-fold smaller than the RP1S (Table 1), yet the RP3U column shows larger or at least competitive retention (Fig. 3). This observed retention behavior and performance is typical of porous polymer monoliths where the retention scales with the phase ratio, i.e. the amount of accessible polymer material in the confine [19]. This is indicated to be largest for the RP3U series (Fig. 2). The pore space, respectively surface area probed in the dry-state is an unsuitable metric as shown with these experiments (Table 1, Figs. 2 and 3). Therefore, the question now arises where the isocratic efficiency of the RP1S column stems from. The probed performance correlates well to that reported by Smirnov et al. [29]. The authors optimized the performance of poly(divinylbenzene-*co*-ethylvinylbenzene-*co*-2-hydroxyethylmethacrylate) monolithic columns in 3 mm I.D. column format [29], while a similar mobile phase composition of acetonitrile/water together with a more hydrophilic monolith was used. They observed, for the best column with readily low permeability and only shown for toluene at much weaker retention (k' = 6), plate heights ranging from H = 40 μm at the smallest linear chromatographic flow velocity to H = 76 μm for a linear chromatographic flow velocity of 2 mm/s [29]. Furthermore, the reported performance in Fig. 5 for the RP1S column is even better than that presented by Causon et al. [47], who measured a plate height generated by the same column of 100 μm for propyl parabene at a column temperature of 80 °C and a retention factor of k' = 3–4 for the lowest flow velocity. The authors used even lower volume percentage of acetonitrile in the mobile phase. This at some point validates that, while the current column performance may appear poor, it is what is typically obtained with tailored systems and its origin to be resolved. The relatively poor performance in all cases may originate from the structural heterogeneity, well known for polymer monoliths [18]. Recently, this aspect was elucidated by numerical simulations of flow through the bulk of a commercial disc monolithic material [48]. The authors physically reconstructed the bulk region of the monolithic material imaged in the dry-state [48]. They further point at the possibility that the heterogeneous macropore space may accommodate varying degrees of convective flow, possibly resulting in large flow dispersion. However, they did not consider the presence of solvent yet, which modulates gel porosity and chromatographically accessible pore space, aggravating this effect for small molecule transport under retentive conditions [18]. Therefore, in the following a focus lies on the data for the measured porosity and phase ratio in pure tetrahydrofuran and 50/50 acetonitrile/water (v/v) as a mobile phase (Table 1). It is obvious, that indeed while moving from the situation of pure tetrahydrofuran in the mobile phase, the porosity and phase ratio are substantially different in 50/50 acetonitrile/water employing uracil with a larger molecular weight than benzene as void marker. While the apparent ε_{total} of the column becomes smaller, the phase ratio increases. The difference is quite significant and again qualitatively the same for all three columns as shown in Table 1. These results point toward difficulties to determine true values of porosity and phase ratio. The monoliths consist of the same base material though obviously prepared under different conditions (Fig. 1). The suspected difference between the scenarios of two solvated-state properties indeed provides guidance for the design of experiments elucidating the elution performance of the porous polymer monoliths. It is realized by utilizing the homologous series of alkylbenzenes that are affected by partition and adsorption (Figs. 3 and 4). Because a change of the phase ratio for small molecules associated with the binary mobile phase solvent mixture composition may provide insight into the modulation of gel porosity, partition and adsorption in a concerted scenario, the height equivalent to a theoretical plate is used as a sensitive means to monitor changes in macroscopic mass transfer efficiency.

3.5. Impact of the volume percentage of acetonitrile modulating gel porosity and retention on performance

Fig. 6a shows example plate height curves for all six retained alkylbenzenes at 60/40 acetonitrile/water (v/v) as the mobile phase spanning retention factors of k' = 5 for benzene to k' = 45 for pentylbenzene. For comparison, the plate height from isocratic elutions was plotted against superficial flow velocity, u_{sf}, as a universal means to exclude impact stemming from varying porosity identified by the variation of phase ratio with the solvent and analytes used (Table 1). In this example, the performance is approximately independent of retention and molecular size at a low superficial velocity while differences are observable for the higher superficial flow velocities (Fig. 6b). It was previously indicated in this work, that retention is governed by the volume percentage of acetonitrile in the mobile phase (Figs. 3 and 4). Varying this concentration of acetonitrile in the mobile phase significantly impacts retention via presumably concerted impact of partition and adsorption. The key question then is what happens to the performance in the elution of small molecules if the content of acetonitrile in the mobile phase is varied. Fig. 7 shows the plate height curves for benzene as the least retained compound (Fig. 7a) and that of pentylbenzene as the strongest retained compound (Fig. 7b). The mobile phase composition was varied from 50/50 acetonitrile/water (v/v) to only acetonitrile. This reflects the retention factor range shown in Fig. 4. Amazingly, in both cases the slope of the plate height curve

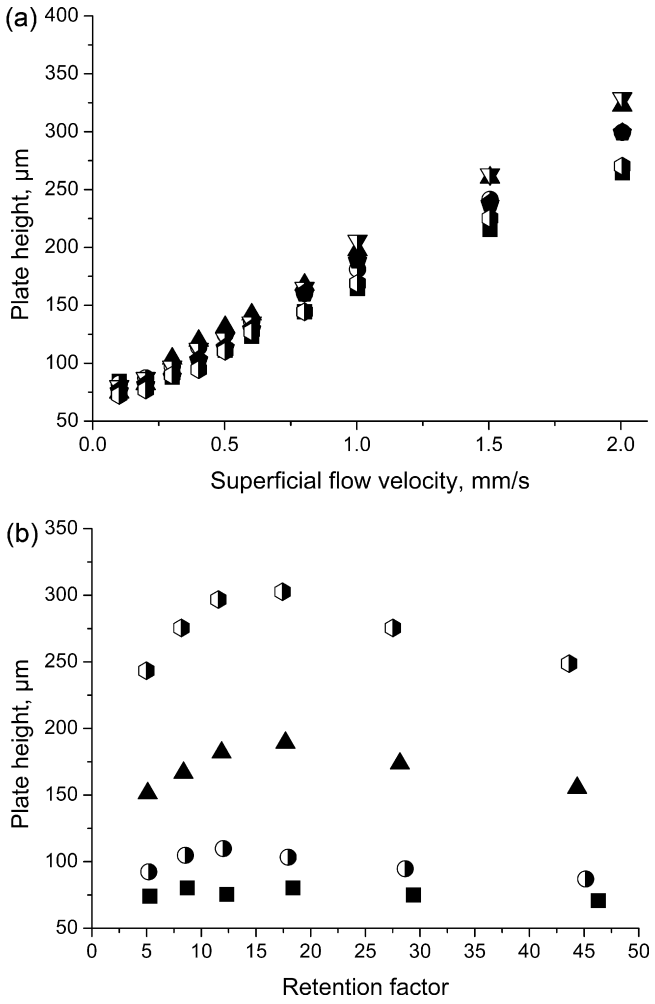

Fig. 6. Performance derived from the isocratic reversed-phase elution of a homologous series of alkylbenzenes on the RP1S column with (a) plate height curves obtained at a mobile phase composition of 60/40 acetonitrile/water (v/v) including benzene (filled squares), toluene (half-filled circles), ethylbenzene (filled triangles), propylbenzene (half-filled triangles), butylbenzene (filled pentagons), and pentylbenzene (half-filled hexagons), and (b) plate heights against retention factor in the homologous series at varying superficial flow velocity of u_{sf} = 0.2 mm/s (filled squares), u_{sf} = 0.4 mm/s (half-filled circles), u_{sf} = 1 mm/s (filled triangles), and u_{sf} = 2 mm/s (half-filled hexagons).

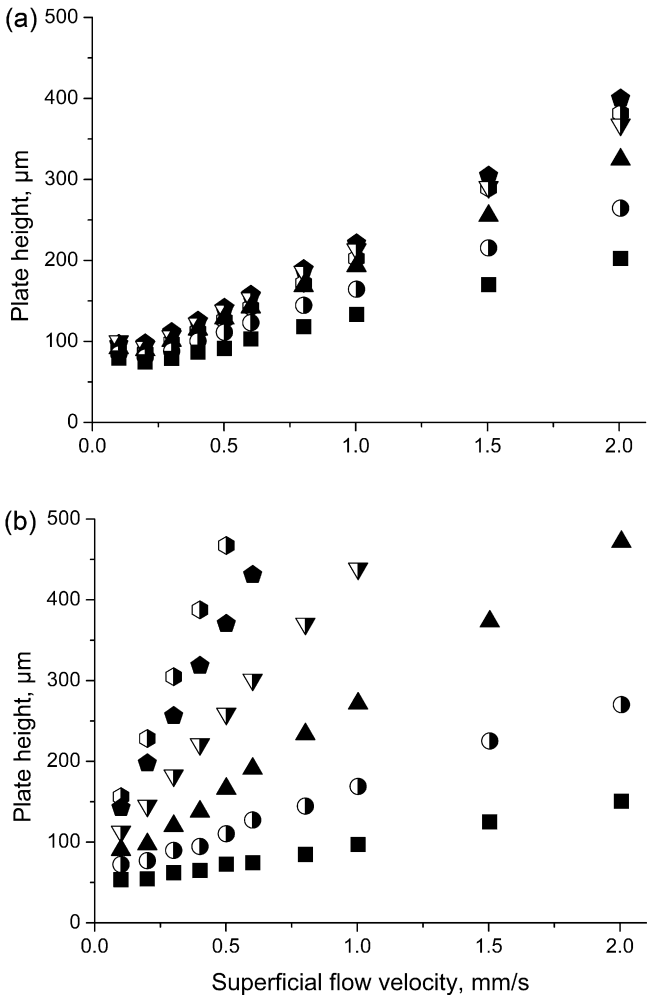

Fig. 7. Plate height curves obtained at varying binary mobile phase compositions for (a) benzene as the smallest eluted compound with lowest retention in the homologous series, and (b) for pentylbenzene as largest compound in the homologous series showing strongest retention and being nearest to the nanopore exclusion limit (Fig. 2b). Volume percentage of acetonitrile in a mixture of acetonitrile/water (v/v): 50% (filled squares), 60% (half-filled circles), 70% (filled triangles), 80% (half-filled triangles), 90% (filled pentagons), 100% (half-filled hexagons).

at increased superficial flow velocity, reflecting stagnant mass transfer resistance in the porous structure, strongly depends on the volume percentage of acetonitrile in the mobile phase. It is further seen that the pentylbenzene (Fig. 7b) is far more sensitive than the smallest eluted analyte benzene (Fig. 7a). It is seen in Fig. 2 that the pentylbenzene is closest to the nanopore exclusion limit in SEC (Fig. 2) and therefore its efficiency may be most sensitive to modulation of gel porosity. Using only acetonitrile as the mobile phase, Fig. 8 then clearly shows that for an increased molecular weight and retention of analytes in the homologous series the plate height is largest for the strongest retained and largest compound in particular at high superficial flow velocities. Interestingly, the curves come closer at low superficial flow velocities. The increased dispersion at increased acetonitrile concentrations (Fig. 7) may simply have its origin in the increased gel porosity at an increased volume fraction of acetonitrile in the mobile phase. At one side it opens the polymer framework providing a higher volume of potentially accessible gel porosity, but at the same time decreases retention based on adsorption as a thermodynamic argument. Indeed, a detailed investigation on all analytes at a superficial flow velocity of u_{sf} = 0.3 mm/s scales with retention in the homologous series

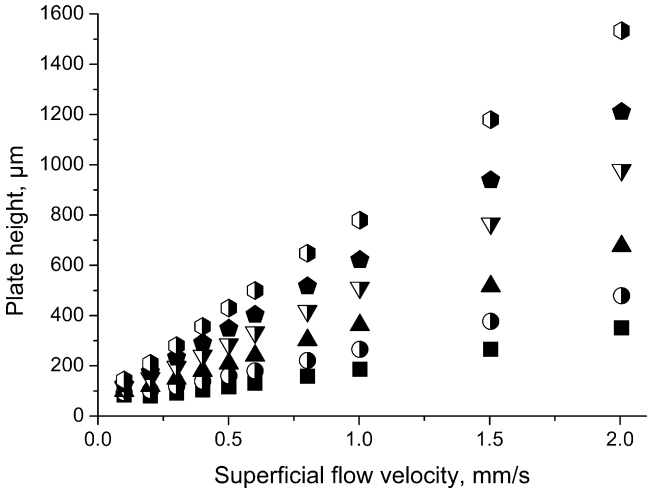

Fig. 8. Plate height curves obtained for acetonitrile as the mobile phase with the RP1S column for benzene (filled squares), toluene (half-filled circles), ethylbenzene (filled triangles), propylbenzene (half-filled triangles), butylbenzene (filled pentagons), pentylbenzene (half-filled hexagons).

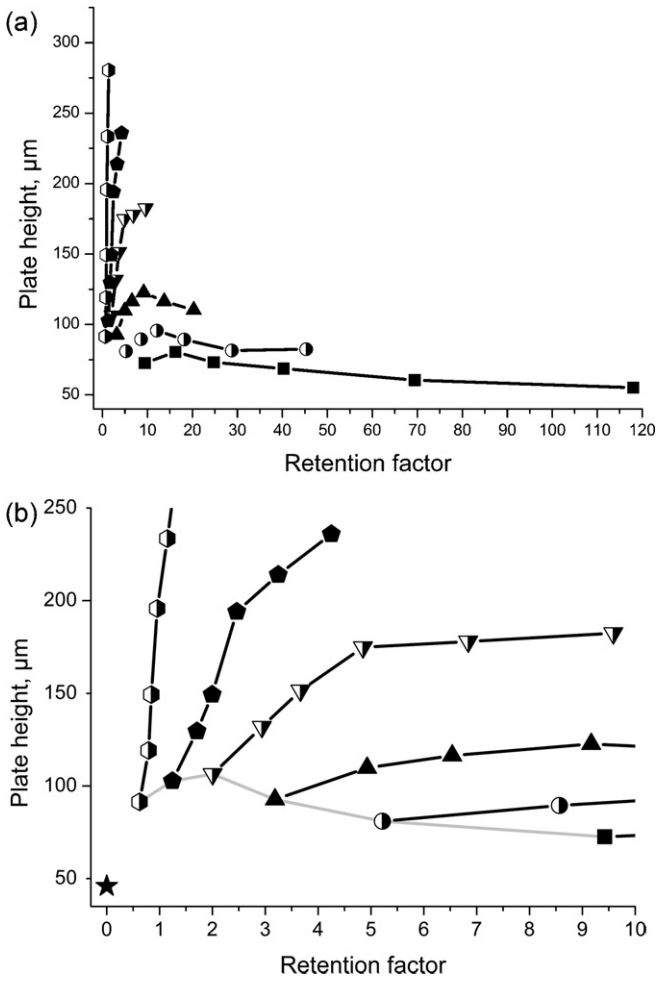

Fig. 9. Effect of size and chromatographic retention of alkylbenzenes on the plate height determined at different volume fractions of acetonitrile in the mobile phase. Superficial flow velocity: u_{sf} = 0.3 mm/s. (a) Entire investigated range of retention factors, and (b) zoom area for a lower retention range including uracil at a mobile phase composition of 50/50 acetonitrile/water (v/v) (filled five-pointed star). Volume percentage of acetonitrile: 50% (filled squares), 60% (half-filled circles), 70% (filled triangles), 80% (half-filled triangles), 90% (filled pentagons), 100% (half-filled hexagons). Connecting gray line in (b) is meant as a guide to the eye for benzene data.

(Fig. 9a). At times this effect has been reported for porous polymer monoliths based on methacrylate chemistries [17,18,20,22] and was indicated with styrene/divinylbenzene chemistries under typical preparatory conditions [19]. This scaling in Fig. 9a becomes most pronounced at the highest volume fraction of acetonitrile in the mobile phase at which still significant retention is discernible (Fig. 3). Plate heights increase with increased retention, realized by an increase in molecular weight of the alkylbenzenes at the given mobile phase composition. This dependence ceases at decreased concentration of acetonitrile in the mobile phase leading to a more retention-insensitive performance at high retention. Here the plate height even slightly decreases with increased retention in the homologous series (Fig. 9a). The plate height for uracil at the same superficial flow velocity and 50/50 acetonitrile/water (v/v) as the mobile phase is shown as filled five-pointed star in Fig. 9b and reflects the best performance. This effect is in agreement to earlier published results with methacrylate-based and styrene/divinylbenzene-based chemistry. It shows that while the performance under kinetic conditions may already be poor [18,19], performance worsens with retention [17–19]. This also contradicts general observation in liquid chromatography practice with silica-based stationary phases [49]. Here, sufficient retention is required to obtain a more realistic view on true column performance since for higher retention factors impact of extra-column contributions to band broadening are reduced to a minimum [49]. Consequently, performance for retained small tracers, are typically better. Also, it was demonstrated before that the efficiency of weakly retained solutes is more sensitive to the radial heterogeneity of columns than that of strongly retained ones [49]. Both analogs however seem to fail with our current experimental results. This points us toward effects which are not ascribed to the heterogeneity in the porous flow-through pore structure in the analytical column format. These results therefore show that indeed nanoscale gel porosity together with partition and adsorption is an important and general phenomenon impacting monolithic polymeric column performance irrespective of their size and format. Minimal effects are seen for the non-retained hydrophilic uracil. If gel porosity is modulated to be large, performance for retained compounds decreases even at reduced retention. This is an indirect evidence of its impact and becomes particularly pronounced at high flow velocity and in the mass transfer dominated regime of the plate height curve (Fig. 8). In other words, a stronger adsorption at reduced gel porosity provides the column with a better performance for retained compounds (Fig. 9b). These results indicate that the unwittingly or deliberately chosen experimental conditions modulate transport efficiency through porous polymer monoliths as a “living” chromatographic support structure. At high volume fractions of acetonitrile in the mobile phase the *C*-Term in the plate height curves scales with the molecular weight of alkylbenzenes, with an increased molecular weight resulting in a lower diffusion coefficient in the gel porosity-breathing polymer matrix (Figs. 8 and 9) since the small molecules permeate it (Fig. 2). In this line performance seems worse for molecules being most close to the nanopore exclusion limit (Fig. 2b).

It is expected that the above-described experiments, their implications and importance should be set in context with the mobile phase composition window where this happens. Therefore, it may be apparent that with variation of the nanoscale stationary phase polymer structure and chemistry, the operational domain and impact of gel-porosity may change. Further, the degree of cross-linking that may determine the overall amount of gel porosity which can be modulated requires consideration, alongside the overall amount of polymer mass in the confine, determining phase ratio. Cautiously spoken, this indicates the fact that the diversity of porous polymer monoliths, which differ only slightly in chemical composition, hydrophilicity, hydrophobicity, phase ratio, etc., as well as characterization performed under different mobile phase compositions and analytes employed, renders direct and quantitative comparisons of performance possibly less adequate.

3.6. Impact of the column temperature on the performance under isothermal conditions

It was shown that gel porosity determines the dispersion dynamics of small-retained tracers in the currently investigated porous polymer monoliths. A stronger manifestation of gel porosity leads to a decrease in performance but most pronounced only under conditions of retention and for molecules that undergo partition and retention phenomena. To directly back-up this impact with a control experiment, high temperature liquid chromatography was used to probe the effect of an enhanced diffusion of these small tracers in the gel porosity region. Shown in Fig. 10 is the performance of the RP1S monolith for strongly retained pentylbenzene. In this chromatographic scenario an increased temperature reduces viscosity of the mobile phase and modulates (additionally to the diffusion coefficient in the moving mobile phase): (i) a reduced retention based on thermodynamic arguments of adsorption [50], and (ii) a postulated enhancement of the

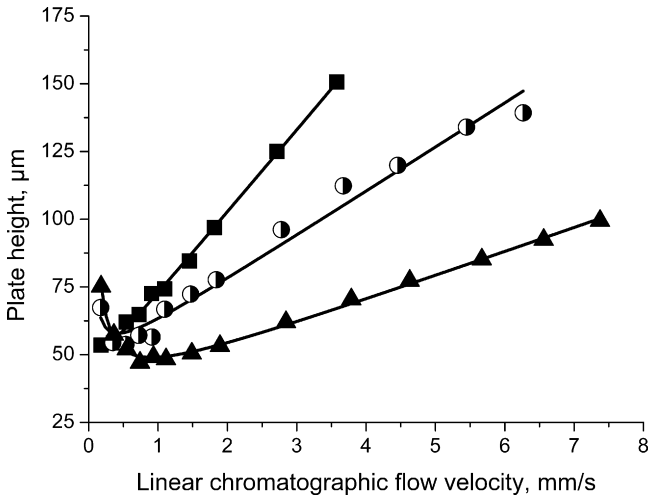

Fig. 10. Impact of isothermal column temperature on the performance of the RP1S series probed with pentylbenzene and expressed as plate height curves fitted with the van-deemter model $H = A + B/u_0 + Cu_0$. A mobile phase composition of 50/50 acetonitrile/water was used. Symbols: 25 °C (filled squares), 50 °C (half-filled circles), and 90 °C (filled triangles).

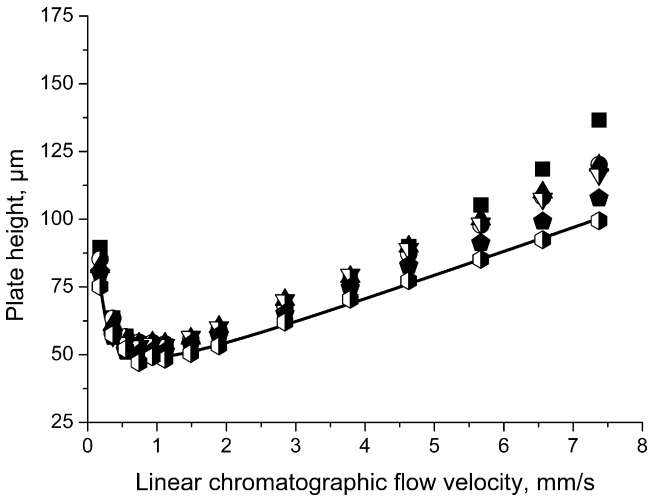

Fig. 11. Plate height curves for the RP1S series at 90 °C isothermal column temperature and a mobile phase composition of 50/50 acetonitrile/water shown for all retained analytes with van-deemter fit ($H = A + B/u_0 + Cu_0$) for pentylbenzene. Symbols: benzene (filled squares), toluene (half-filled circles), ethylbenzene (filled triangles), propylbenzene (half-filled triangles), butylbenzene (filled pentagons), pentylbenzene (half-filled hexagons).

diffusion of the analyte in the polymeric matrix which becomes permeated by (hindered) diffusion. It can be seen that a barely measurable minimum plate height for this strongly retained tracer leads at increased temperature to a more defined minimum at increased mobile phase velocities. Interestingly, the plate height at very low linear chromatographic flow velocities increases due to an enhanced axial diffusion [50]. The curves also show that indeed the inherently poor mass transfer kinetics in the polymer globule matrix based on partition and adsorption is enhanced by increasing temperature. Temperature accelerates the kinetics of transport. This becomes pronounced at linear chromatographic flow velocities exceeding those of 0.5–1 mm/s. It is due to a decrease in the mass-transfer resistance originating from hindered diffusive mass transfer in the polymer gel matrix. Further, no significant improvement in the overall achievable minimum plate height is achieved, which again hints toward the fact that the poorly structured macropore space and associated flow heterogeneity provides a bias somewhat only partly responsible for the observed poor performance in the elution of retained small analytes [18]. For retained small molecules, rather gel porosity and its varying impact that deteriorates performance seems a major issue [17,18]. Fig. 11 shows the performance obtained from elution of all the analytes at a temperature of 90 °C and varying linear chromatographic flow velocities. A minimum plate height of approximately 45–50 μm is observed for all analytes. The *C*-Term of retained pentylbenzene amounts 9 ms under such rather extreme conditions. Fig. 12 shows the performance of polymer monoliths in the separation of a homologous series of alkylbenzenes at 1.9 mm/s, 3.8 mm/s, and 7.5 mm/s performed at 90 °C column temperature, an intermediate temperature value as that probed by Causon et al. for a single small molecule, [47] but with much higher linear chromatographic flow velocities in the current work. Indeed, the homologous series can still be resolved at this high linear chromatographic flow velocity and strong retention thanks to the much reduced *C*-Term contribution to the plate height. Expectedly, the efficiency is very decent in the mass transfer dominated regime (Fig. 11).

4. Discussion

An experimental study of the porous and hydrodynamic properties of analytical scale column format poly(styrene-*co*-divinylbenzene) monolithic scaffolds is reported. The current study focuses on three different metric properties that are: (i) the columns dry-state porous properties (Fig. 1 and Table 1), (ii) the gel porosity probed by SEC using a range of narrow molecular weight distribution PS standards and small sub-nanometer-sized solutes in tetrahydrofuran (Fig. 2), as well as (iii) correlation of hydrodynamic dispersion to the porous structure (Fig. 5), modulated gel porosity and analyte size (Figs. 7–9). Considering all metric properties accessible by the most simple and straightforward dry-state and chromatographic measurements of identical material, the following findings can be summarized. As a most fundamental property, it is apparent that the polymer monoliths exhibit a significant amount of gel porosity irrespective investigations of dry-state porous properties (Figs. 1 and 2, Table 1). Associated with this gel-porosity is the existence of nanometer-sized pore space beyond that shown by typical dry-state investigations making such determinations an unsuitable metric for explanation of the monoliths performance. Performance varies with mobile phase solvent composition, consequently retention and partition (Figs. 3, 4, 7 and 9). This variation

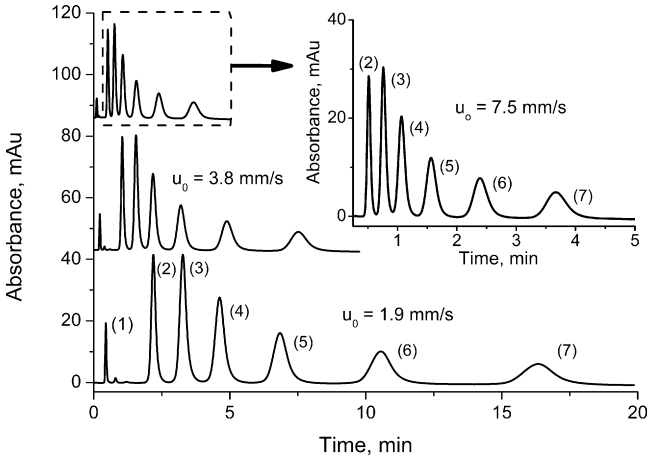

Fig. 12. Separation of a homologous series of alkylbenzenes including (1) Uracil, (2) benzene, (3) toluene, (4) ethylbenzene, (5) propylbenzene, (6) butylbenzene, (7) pentylbenzene at a column temperature of 90 °C, a mobile phase composition of 50/50 acetonitrile/water (v/v), and varying linear chromatographic flow velocities.

of the reversed-phase chromatographic performance in the isocratic separation of small molecules, which depends on analyte size and retention, becomes modulated by varying binary mobile phase solvent composition (Figs. 7 and 9). It is therefore most likely to change with changing solvent and stationary phase chemistry. This also means that the reported performance of polymer monoliths may mostly depend on polymer backbone chemistry and employed solvent, making comparison of the performance between different laboratories less adequate. Even slightly different experimental conditions for preparation and characterization cause this issue.

With respect to these commonalities the specifically employed preparatory conditions can result in the following differences which provide interesting incentives for further research and tailoring of performance, beyond that for which these materials are designed. It is clear that all three columns show a different macroporous flow-through pore structure, with the finest structure provided by the RP1S series, larger globular structure of the RP2H series and the pronounced large globular structure of the RP3U series (Fig. 1). Associated with the difference in the globular morphology and possibly also the cross-link density, the materials also show significantly different dry-state surface area (Table 1). Therefore, the size of the globular features affects stagnant mass transfer resistance and hydrodynamic dispersion via the existent microporous/mesoporous globular structure in the solvated-state (Figs. 1 and 2). This is similar to that provided by a packed bed of porous adsorbent particles, however, with a more rigid and permanent mesoporous structure of hard silica matter and of course a different flow-through-pore morphology. It becomes clear from Figs. 1 and 5 that large globular features provide a larger diffusion distance inside the macropore confining polymer which changes additionally with mobile phase solvent composition and presumably cross-link density distribution. Therefore, these results show that small globular features are favorable (Figs. 1 and 5). These can also be obtained by an incomplete polymerization reaction. An incomplete polymerization results in an overall higher amount of porosity and therefore reduced gel porosity [18,19]. The size of stagnant intra-globule mass transfer zones associated with the size of the globules therefore needs to be reduced. Furthermore, the globule scale cross-link density distribution, recently discussed in the literature [17], requires attention. Alternatively, a permanent mesoporous globule structure may be created during preparation. A permanent mesoporous globule structure may also reduce gel porosity as a consequence of an increase in overall existent porosity. This was indicated with bead-based porous systems [36] and monoliths [19]. This is in analogy to a reduced phase ratio (Table 1). It should be kept in mind that the total amount of accessible polymeric mass needs to be controlled after deduction on where it is located. For example, in a monolith with smaller feature size, existent gel layers [35] and permeable polymeric mass [36,37] as indicated previously for porous monoliths [17], and also shown in this work (Fig. 2), may have less impact than in monoliths with larger globule size. It is suspected, that in the large globular structures a larger diffusion distance as e.g. in the RP3U series (Fig. 1a) is probed in chromatography of small molecules (Fig. 5). This would be in analogy to that of an increased particle size in a particulate bed. In the current case it totally deteriorates performance since the *C*-Term approaches values beyond being acceptable (Fig. 5). Further, the gel porosity seems most pronounced when the globules appear almost non-porous in their dry-state hinting toward a low degree of cross-linking (Figs. 1a and 2, Table 1). While it appears logic, that the impact of the modulated gel porosity and related partition phenomena may vary in all three columns, though fundamentally having the same origin, it also confirms earlier conclusion on studies of the porous and hydrodynamic properties of capillary-scale format columns, that gel porosity needs to be reduced to reduce band broadening [18,19]. For that aspect, a reduced phase ratio and globule size of which the polymeric backbone is composed may provide a possible improvement in performance. This is somewhat independent of the flow-heterogeneity originating from varying flow-through pore sizes in the columns. Wall effects, not considered in this work, certainly require separate investigations. Ultimately, a reduction in feature size and increase in number of flow-through pores at the cost of a reduced permeability may therefore be an interesting option for tailoring column performance. Systematic studies yet have to be performed.

5. Conclusions

Results presented in this study confirm initial anticipations derived from experiments in capillary-sized molds that the hydrodynamic properties of porous polymer monoliths are governed largely by the existent gel porosity in monolithic scaffolds [18]. This is directly addressed for a set of analytical column scale format porous polymer monoliths for the first time. It is suspected that gel porosity is a phenomenon which obscures chromatographic performance of porous polymer monoliths in all conduit sizes and shapes and that miniaturization cannot mediate for these effects. Results presented in this study show that gel porosity may dominate the dispersion and retention dynamics of porous monolithic scaffolds unambiguously. This is even with respect to improved performances that may be and are obtained due to tailored preparatory conditions resulting in a much improved morphology and smaller feature sizes. Improved performances in miniaturized column formats may thereby be a consequence of the more homogenous (but random) radial porous structure within certain ranges of size and the better system adoptability resulting in a reduction of chromatographic band dispersion. This is due to the *A*-Term, reflecting flow heterogeneity, which is poor and commonly well known for polymer monoliths. Recent efforts have already demonstrated that monoliths possess great miniaturization potential and due to the smaller dimensions a better control of porous flow-through properties may be achieved. However, only quantitative differences from mass transfer resistance contributions may be expected. They principally originate from the base material property.

Again, it was attempted to characterize the impact of gel porosity on the hydrodynamic dispersion of small-sized solutes with a set of selected available columns designed for and showing excellent performance in large molecule applications in non-equilibrium elution mode. We are currently working on characterizing the impact of gel porosity on larger analytes since the results obtained so far indicate that gel porosity may impact dispersion dynamics of larger molecular species aside from effects stemming from flow heterogeneity. A diminished contribution to hydrodynamic dispersion may be due to the generally lower amount of organic modifier employed in reversed-phase gradient elution mode of bio-macromolecules, thereby resulting in conditions suppressing gel porosity. The larger size of proteins of at least single or several nanometers may therefore make them less sensitive to the nanoscale polymer structure but this has not been addressed so far. An additional aspect is that associated effects may be buried under gradient elution data realized in non-equilibrium liquid chromatography.

With respect to all the presented effects it would be rewarding to study the impact of molecular size, retention, and mobile phase composition on the performance of porous polymer monoliths as most pivotal tools modulating material characteristics. It is advisable to always report the performance and retention for all analytes observed in the chromatogram. We might discover that by wittingly modifying experimental conditions and by performing a related analysis of transport performance, the current picture of porous polymer-based separation media will be refined. In the course of discovering the founding elements of their

performance, the demand for better performance can become a demand directed into more realistic goals. Any apparent improvements should be based on tailored material characteristics of such adjustably performing chromatographic materials and not specific liquid chromatography conditions, format shapes and sizes, or associated random lucks in preparatory conditions.

Acknowledgements

The author acknowledges experimental support from Antonia Praus at the Institute of Polymer Chemistry, Johannes Kepler University Linz as a dedicated lab assistant and Günter Hesser for scanning electron microscopy measurements at the Center for Surface and Nanoanalytics (ZONA) at Johannes Kepler University Linz. Prof. Wolfgang Buchberger at the Institute of Analytical Chemistry, Johannes Kepler University Linz is acknowledged for fruitful discussions. Kelly Flook from Thermo Fisher Scientific (Sunnyvale, California) is acknowledged for the generous gift of the columns, without which this study would not have been possible.

References

[1] S. Hjerten, J.L. Liao, R. Zhang, J. Chromatogr. 473 (1989) 273.
[2] T.B. Tennikova, M. Bleha, F. Svec, T.V. Almazova, B.G. Belenkii, J. Chromatogr. 555 (1991) 97.
[3] Q.C. Wang, F. Svec, J.M.J. Fréchet, Anal. Chem. 65 (1993) 2243.
[4] A. Premstaller, H. Oberacher, C.G. Huber, Anal. Chem. 72 (2000) 4386.
[5] H. Oberacher, C.G. Huber, Trac-Trends Anal. Chem. 21 (2002) 166.
[6] P. Pruim, M. Öhman, Y. Huo, P.J. Schoenmakers, W.T. Kok, J. Chromatogr. A 1208 (2008) 109.
[7] A. Jungbauer, R. Hahn, J. Chromatogr. A 1184 (2008) 62.
[8] M.H.M. van de Meent, S. Eeltink, G.J. de Jong, Anal. Bioanal. Chem. 399 (2011) 1845.
[9] J. Rozenbrand, W.P. van Bennekom, J. Sep. Sci. 34 (2011) 1934.
[10] F. Svec, T.B. Tennikova, Z. Deyl (Eds.), Monolithic Materials: Preparation, Properties, and Applications, Elsevier, Amsterdam, 2003.
[11] F. Svec, J. Chromatogr. A 1217 (2010) 902.
[12] I. Nischang, O. Brueggemann, F. Svec, Anal. Bioanal. Chem. 397 (2010) 953.
[13] A.R. Ivanov, L. Zang, B.L. Karger, Anal. Chem. 75 (2003) 5306.
[14] I. Nischang, F. Svec, J.M.J. Fréchet, Anal. Chem. 81 (2009) 7390.
[15] R. Bakry, G.K. Bonn, D. Mair, F. Svec, Anal. Chem. 79 (2007) 486.
[16] H. Aoki, N. Tanaka, T. Kub, K. Hosoya, J. Sep. Sci. 32 (2009) 341.
[17] I. Nischang, I. Teasdale, O. Brüggemann, Anal. Bioanal. Chem. 400 (2011) 2289.
[18] I. Nischang, O. Brüggemann, J. Chromatogr. A 1217 (2010) 5389.
[19] I. Nischang, I. Teasdale, O. Brüggemann, J. Chromatogr. A 1217 (2010) 7514.
[20] D. Moravcova, P. Jandera, J. Urban, J. Planeta, J. Sep. Sci. 26 (2003) 1005.
[21] P. Coufal, M. Cihak, J. Suchankova, E. Tesarova, Z. Bosakova, K. Stulik, J. Chromatogr. A 946 (2002) 99.
[22] Y. Huo, P.J. Schoenmakers, W.T. Kok, J. Chromatogr. A 1175 (2007) 81.
[23] Q.C. Wang, F. Svec, J.M.J. Fréchet, J. Chromatogr. A 669 (1994) 230.
[24] Z.D. Xu, L.M. Yang, Q.Q. Wang, J. Chromatogr. A 1216 (2009) 3098.
[25] A. Greiderer, S.C. Ligon, C.W. Huck, G.K. Bonn, J. Sep. Sci. 32 (2009) 2510.
[26] S.H. Lubbad, M.R. Buchmeiser, J. Chromatogr. A 1217 (2010) 3223.
[27] J. Urban, F. Svec, J.M.J. Fréchet, J. Chromatogr. A 1217 (2010) 8212.
[28] Y.Y. Li, H.D. Tolley, M.L. Lee, J. Chromatogr. A 1218 (2011) 1399.
[29] K.N. Smirnov, I.A. Dyatchkov, M.V. Telnov, A.V. Pirogov, O.A. Shpigun, J. Chromatogr. A 1218 (2011) 5010.
[30] S. Shu, H. Kobayashi, N. Kojima, A. Sabarudin, T. Umemura, J. Chromatogr. A 1218 (2011) 5228.
[31] A. Podgornik, J. Jancar, M. Merhar, S. Kozamernik, D. Glover, K. Cucek, M. Barut, A. Strancar, J. Biochem. Biophys. Methods 60 (2004) 179.
[32] A. Podgornik, J. Jancar, I. Mihelic, M. Barut, A. Strancar, Acta Chim. Slov. 57 (2010) 1.
[33] I. Nischang, F. Svec, J.M.J. Fréchet, J. Chromatogr. A 1216 (2009) 2355.
[34] G. Guiochon, J. Chromatogr. A 1168 (2007) 101.
[35] K. Jerabek, Anal. Chem. 57 (1985) 1598.
[36] F. Nevejans, M. Verzele, Chromatographia 20 (1985) 172.
[37] F. Nevejans, M. Verzele, J. Chromatogr. 406 (1987) 325.
[38] W. Mandema, H. Zeldenrust, Polymer 18 (1977) 835.
[39] J.Y. Li, L.M. Litwinson, F.F. Cantwell, J. Chromatogr. A 726 (1996) 25.
[40] J.Y. Li, F. Cantwell, J. Chromatogr. A 726 (1996) 37.
[41] B. Ells, Y. Wang, F.F. Cantwell, J. Chromatogr. A 835 (1999) 3.
[42] D. Bolliet, C.F. Poole, Chromatographia 46 (1997) 381.
[43] F. Gritti, A. Felinger, G. Guiochon, J. Chromatogr. A 1136 (2006) 57.
[44] A. Vailaya, C. Horvath, J. Chromatogr. A 829 (1998) 1.
[45] J.L. Rafferty, J.I. Siepmann, M.R. Schure, J. Chromatogr. A 1218 (2011) 2203.
[46] C.F. Poole, S.K. Poole, J. Chromatogr. A 1216 (2009) 1530.
[47] T.J. Causon, R.A. Shellie, E.F. Hilder, J. Chromatogr. A 1217 (2010) 3765.
[48] H. Koku, R.S. Maier, K.J. Czymmek, M.R. Schure, A.M. Lenhoff, J. Chromatogr. A 1218 (2011) 3466.
[49] F. Gritti, G. Guiochon, J. Chromatogr. A 1217 (2010) 6350.
[50] T. Greibrokk, T. Andersen, J. Chromatogr. A 1000 (2003) 743.